# Remote Control of Respiratory Neural Network by Spinal Locomotor Generators

Jean-Patrick Le Gal, Laurent Juvin, Laura Cardoit, Muriel Thoby-Brisson, Didier Morin*

Institut de Neurosciences Cognitives et Intégratives d'Aquitaine, CNRS, University of Bordeaux, Bordeaux, France

## Abstract

During exercise and locomotion, breathing rate rapidly increases to meet the suddenly enhanced oxygen demand. The extent to which direct central interactions between the spinal networks controlling locomotion and the brainstem networks controlling breathing are involved in this rhythm modulation remains unknown. Here, we show that in isolated neonatal rat brainstem-spinal cord preparations, the increase in respiratory rate observed during fictive locomotion is associated with an increase in the excitability of pre-inspiratory neurons of the parafacial respiratory group (pFRG/Pre-I). In addition, this locomotion-induced respiratory rhythm modulation is prevented both by bilateral lesion of the pFRG region and by blockade of neurokinin 1 receptors in the brainstem. Thus, our results assign pFRG/Pre-I neurons a new role as elements of a previously undescribed pathway involved in the functional interaction between respiratory and locomotor networks, an interaction that also involves a substance P-dependent modulating mechanism requiring the activation of neurokinin 1 receptors. This neurogenic mechanism may take an active part in the increased respiratory rhythmicity produced at the onset and during episodes of locomotion in mammals.

## Introduction

Upon initiation of exercise or locomotion, breathing rate rapidly increases in anticipation of the subsequent increased oxygen demand. Peripheral chemoreceptors provide one of the most important inputs for breathing regulation. However, chemoreception cannot account for this initial increase, because carbon dioxide and oxygen levels in the blood remain relatively constant at the onset of physical exertion [1,2]. It is now widely recognized that the increase in respiratory rate observed at the onset of exercise, and sometimes even before exercise [3,4], is mainly influenced by neural mechanisms [5,6]. For instance, central commands originating either from the hypothalamic [7,8], the mesencephalic [9], or the pontomedullary [10] locomotor region produce episodes of locomotion that are associated with a marked increase in respiratory activity. Thus, such feedforward mechanisms efficiently contribute to the increase in ventilation during exercise.

The rapid adjustment of breathing rate during exercise also involves muscular sensory feedback mechanisms. Known to be rhythmically activated during episodes of locomotion [11,12], spinal peripheral afferents arising from limb muscle proprioceptors can promptly reset and entrain respiratory rhythmicity [13–18]. Indeed, cyclic activation of spinal sensory inputs is involved in the coupling between locomotor and respiratory rhythms in several species [19], and could also contribute to the exercise-induced increase in respiratory rate.

These feedforward and feedback mechanisms for functional interactions between respiratory and locomotor networks contribute to the functional coupling between breathing and locomotor behaviors. However, another attractive hypothesis would be to consider that direct influence from the locomotor central pattern generator (CPG) to the respiratory CPG would also constitute an optimal neurogenic mechanism, which would permit efficient and reliable adjustment of the respiratory CPG excitability. To test the existence of this previously unreported mechanism, we used an isolated *in vitro* brainstem-spinal cord preparation from neonatal rats [20]. This reduced preparation retains the capacity to generate both spontaneous respiratory rhythmicity originating from the medulla and pharmacologically induced locomotor rhythm produced in the lumbar spinal cord, thus allowing investigating potential direct interactions between the two central motor rhythm-generating networks. Here, we show that pharmacological activation of lumbar locomotor generator increases respiratory frequency. This effect requires the functional integrity of the parafacial respiratory group (pFRG) network and is mediated through a modulatory pathway dependent on substance P (SP). Furthermore, the increase in respiratory frequency observed during fictive locomotion is associated with a tonic depolarization of pre-inspiratory (Pre-I) neurons of the pFRG. Thus, our results assign the pFRG/Pre-I neurons a new role as relays in the pathway through which lumbar CPGs stimulate the medullary respiratory network during locomotion.

## Materials and Methods

### Newborn rat lines and care

All surgical and experimental procedures conformed to the guidelines of the European Communities Council Directive and
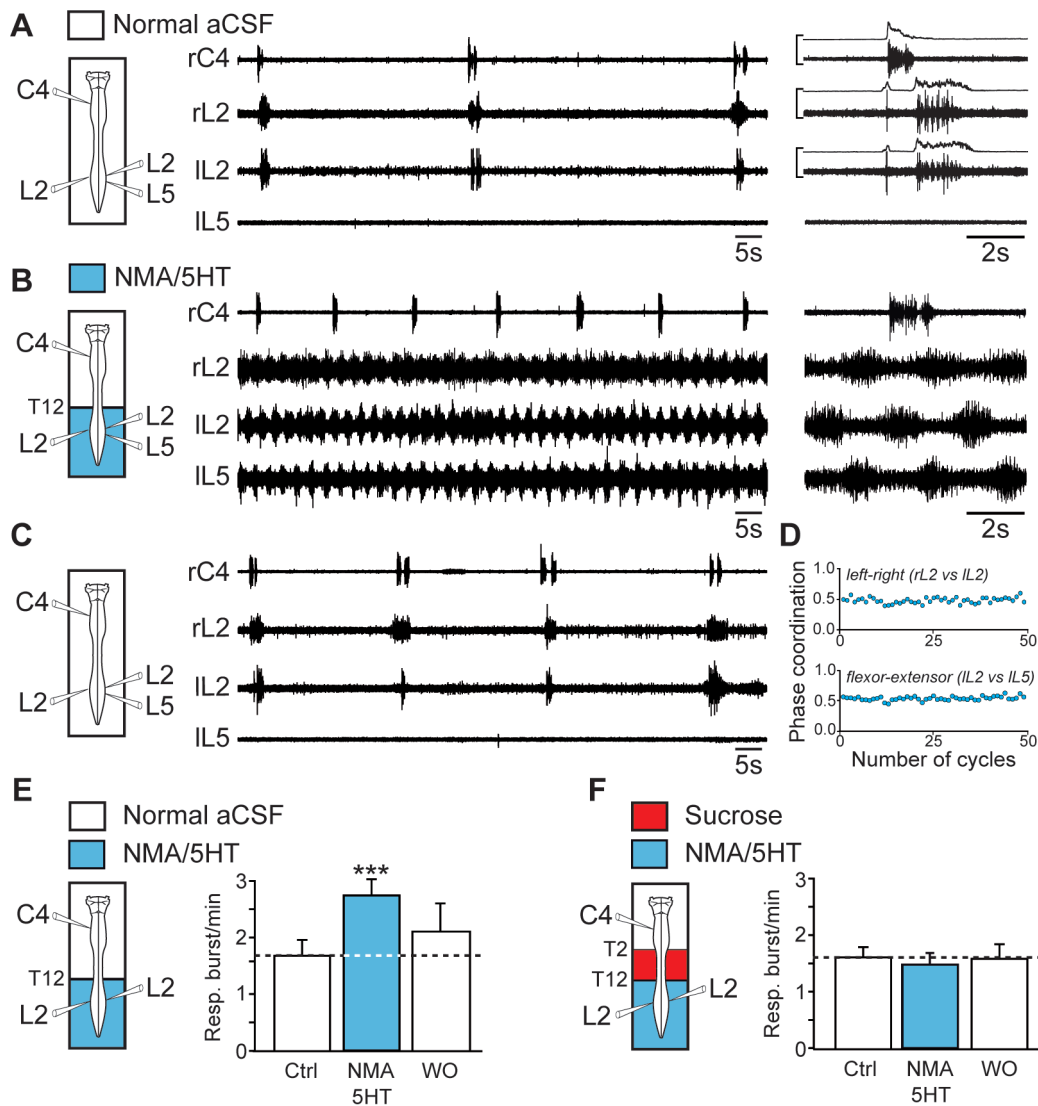
**Figure 1. Activation of the hindlimb locomotor CPG increases the respiratory burst frequency.** A, *left*, Schematic of the experimental procedure. *middle*, Raw spontaneous respiratory activity recorded from cervical (C4, inspiratory-like) and left (l) and right (r) lumbar (L2, expiratory-like) ventral roots. Note that under the control conditions, L5 motor output remained silent. *right*, Expanded traces of averaged integrated (9 sweeps) and raw activity recorded from the same ventral roots. B, Increase of the respiratory burst frequency during NMA/5HT-induced fictive locomotion (schematic at left). The layout is the same as that in (A). Expanded traces of the respiratory and locomotor bursts recorded from cervical (C4) and lumbar (L2 and L5) ventral roots, respectively, are shown at right. C, Recordings of respiratory activity during wash-out of NMA/5HT (schematic at left). D, Time course of the left–right (right L2 versus left L2, top) and flexor–extensor (left L2 versus left L5, bottom) phase coordination during fictive locomotion. Recordings and analysis shown in A to D are from the same preparation. E, F, *left*, Schematics of experimental setup. *right*, Bar charts showing the spontaneous respiratory burst frequency (mean ± SEM) under control (Ctrl) saline conditions (left, open bar), during NMA/5HT application to the lumbar region (blue bar), and during NMA/5HT wash-out (WO; right, open bar) when the lumbar segments of the cord were connected to the upper spinal and brainstem regions (E, n = 14 preparations) or disconnected by sucrose blockade of the thoracic (T2–T12) segments (F, n = 7 preparations). ***$P < 0.001$ (repeated measures ANOVA, Tukey's post hoc tests).
doi:10.1371/journal.pone.0089670.g001

## *In vitro* isolated brainstem–spinal cord preparation

Neonatal rats (P0–2) were deeply anesthetized by hypothermia and decapitated. The skin and muscles were rapidly removed, and the preparation was then placed in a 25-ml recording chamber containing circulating artificial cerebrospinal fluid (aCSF) maintained at 10°C. The spinal cord with its dorsal and ventral roots still attached was isolated by dissection under a binocular microscope. The brainstem–spinal cord preparation was fixed on a Sylgard resin block with the ventral surface upward. Preparations were superfused continuously with aCSF (pH 7.4) equilibrated with 95% $O_2$ and 5% $CO_2$ and containing the following (concentrations in mM): NaCl 100, KCl 4, $NaH_2PO_4$ 1.2, $CaCl_2$ 2, $MgCl_2$ 1.3, $NaHCO_3$ 25, and D-glucose 30. At the end of the dissection, the temperature of the bathing medium was progressively raised to 22–25°C before recordings began. This aCSF
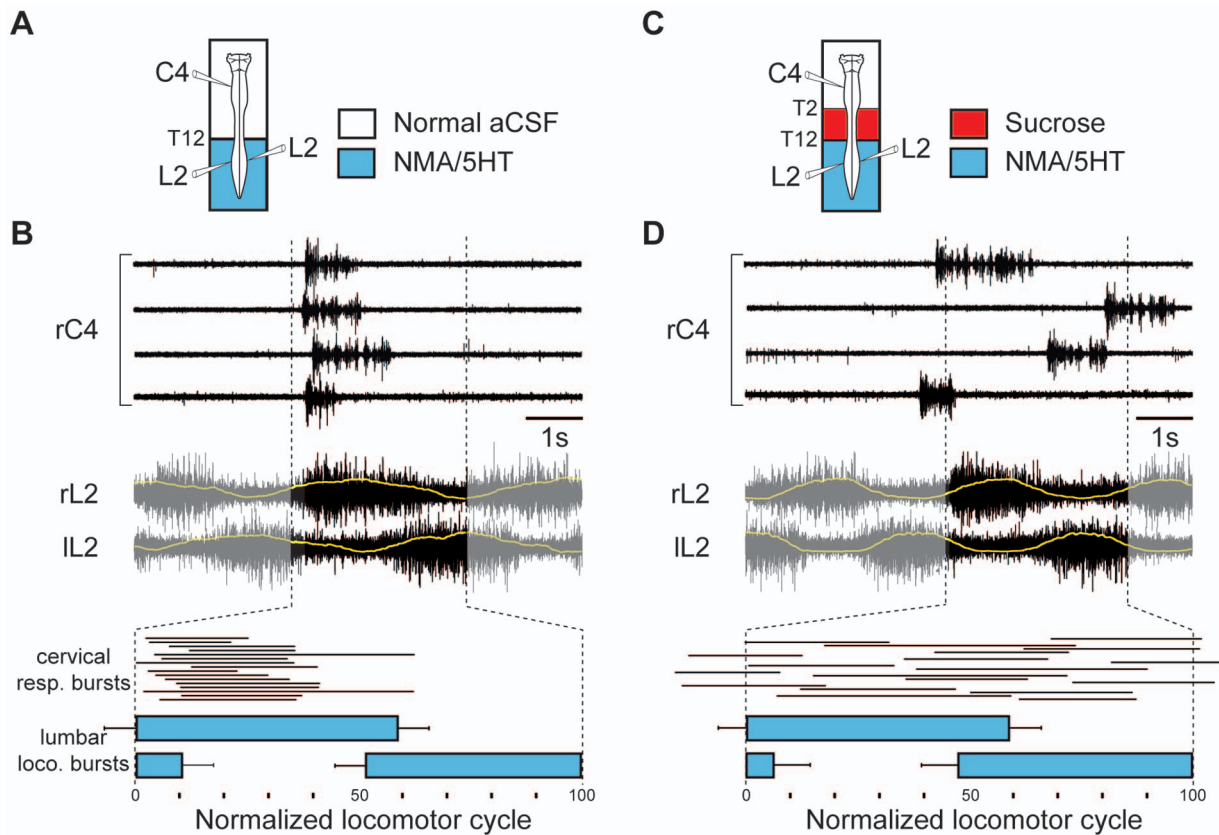
**Figure 2. Phase relationship between respiratory and locomotor bursts.** A, C, Schematics of experimental setup. B, D, *upper and middle traces*, Raw respiratory and locomotor activity recorded from right cervical (rC4) and left-right lumbar (rL2 and lL2) ventral roots, respectively, when lumbar spinal region was connected to the upper spinal and brainstem structures (B) or disconnected by a sucrose blockade of thoracic segments (D). Yellow lines superimposed on rL2 and lL2 discharges are an averaging (30 successive locomotor cycles) of integrated locomotor ventral root activity. *lower diagrams*, Phase diagrams illustrating normalized locomotor step cycles during pharmacologically evoked fictive locomotion. Note that cervical respiratory (resp.) bursts (thin horizontal lines) occur preferentially in-phase with lumbar locomotor (loco.) discharges (blue horizontal bars) when hindlimb locomotor CPG are connected to the medullary respiratory generators (B). Recordings and analysis shown in B and D are from the same preparation.
doi:10.1371/journal.pone.0089670.g002

solution is commonly used to study the operation of locomotor rhythm-generating networks in isolated spinal cord preparation [21–24]. In these conditions, however, the elevated extracellular concentration of calcium (2 mM) induces a low baseline respiratory rate as observed in our experiments [25,26]. Nevertheless, this reduced excitability is required to simultaneously record inspiratory- and expiratory-related motor activities for more than 2.5 hours (time necessary to achieve some of our protocols).

### Electrophysiological recording and stimulation

Motor output activity in spinal ventral roots and pFRG network bursting were recorded with glass suction electrodes filled with aCSF solution. Signals were amplified (10,000 times) by differential AC amplifiers (low cutoff, 100 Hz; high cutoff, 1 kHz; model 1700; A-M Systems), digitized and acquired via a CED 1401 interface, stored on a computer, and analyzed using Spike2 software (Cambridge Electronic Design).

Patch-clamp recordings of pFRG cells were made in whole-cell current clamp mode. Electrophysiological signals were recorded with an Axoclamp-2A amplifier (Molecular Devices), a digitizing interface (Digidata 1322A; Molecular Devices), and pCLAMP 10 software (Molecular Devices). Pipettes were pulled to a tip resistance of 5–7 M$\Omega$ and filled with solution containing (concentrations in mM) potassium gluconic acid 140, $CaCl_2 \cdot 6H_2O$

1, EGTA 10, $MgCl_2$ 2, $Na_2ATP$ 4, Hepes 10, and 0.1% biocytin. The pH was adjusted to 7.2.

Sacrocaudal dorsal roots were stimulated (30 pulses, 1 Hz, 0.5–1 V) via glass suction electrodes with a Master-8 simulator (A.M.P.I) controlled by software written in our laboratory.

### Drug application

Pharmacological substances were bath-applied at least 30 min after the end of the dissection. When required, the recording chamber was partitioned either into 2 or 3 compartments with barriers of syringe-ejected Vaseline to permit differential exposure of selected spinal cord regions to pharmacological treatment. The watertightness of the partitions was systematically checked at the end of the experiment by verifying that methylene blue added to one side of the Vaseline bridge did not leak into the other side. Experiments in which leakage was observed were discarded.

A mixture of $N$-methyl-D,L-aspartate (NMA; 15 µM; Sigma) and serotonin (5HT; 15 µM; Sigma) was applied to lumbar segments to elicit prolonged and stable episodes of fictive locomotion. In some cases, a sucrose solution (10%) or a modified aCSF solution in which the $Ca^{2+}$ and $Mg^{2+}$ concentrations were lower and higher, respectively, than those in the normal aCSF solution (0.1 mM $CaCl_2$ and 5 mM $MgCl_2$ *vs* 2 mM $CaCl_2$ and 1.3 mM $MgCl_2$) was bath-applied to the thoracic or cervical compartment
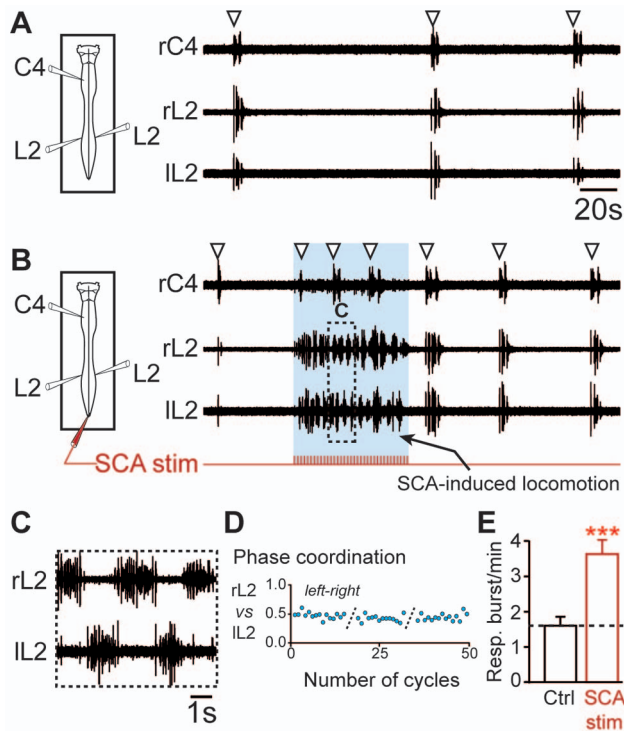
**Figure 3. Electrical stimulation of SCA activates the lumbar locomotor CPG and increases the respiratory rate.** A, *left*, Schematic of experimental procedure. *right*, Spontaneous respiratory activity from cervical (C4) and right (r) and left (l) lumbar (L2) ventral roots. White arrowheads denote detected respiratory bursts. B, Fictive locomotion and increase in respiratory burst frequency induced during the tonic stimulation of SCA. The layout is the same as that in (A). Expanded traces of fictive locomotor burst activity recorded from bilateral L2 ventral roots in (B). D, Plot showing left-right locomotor phase coordination occurring between bilateral flexor (L2) ventral roots during 3 successive episodes of SCA stimulation–induced locomotion. E, Bar charts illustrating changes in respiratory burst frequency (Resp.; mean ± SEM; n = 7 preparations) following SCA stimulation. Recordings and analysis shown in A to D are from the same preparation. Ctrl, control. *** P<0.001 (Student's paired *t* test).
doi:10.1371/journal.pone.0089670.g003

to reversibly block axonal conduction or all chemical synaptic transmission [27], respectively.

The neurokinin 1 receptor (NK1R) antagonist spantide (Sigma) was applied to the brainstem region at a concentration of 5 µM. The preparation was pre-incubated in spantide for 1 h [28].

## Brainstem transection and lesion

Serial transverse sectioning of the brainstem was performed with a scalpel blade. To determine the involvement of brainstem structures in the locomotion-induced accelerated respiration, we transected the preparation rostral to the anterior inferior cerebellar artery (AICA) or we performed mechanical focal lesions of the brainstem with the tip of a glass suction electrode. The axial level of the transections (or lesions) was later anatomically verified on a parasagittal section of the brainstem.

## Histology

Following a transection or a lesion, the brainstem was stained for choline acetyltransferase. The tissue was fixed overnight at 4°C in 4% paraformaldehyde in PBS (0.1 M) and then rinsed twice in PBS and cryoprotected with 20% sucrose in PBS overnight. After

the tissue was embedded in Tissue Tek and frozen to −80°C with cooled isopentane, 30-µm-thick serial parasagittal sections were cut on a cryostat. Free-floating sections were rinsed in PBS 3 times (each rinse lasted 10 min), saturated with PBS, Triton X100 0.3%, and BSA 1%, and incubated with a goat anti-choline acetyltransferase polyclonal antibody (1:100, Millipore) for 18 h at room temperature (RT). Then the sections were rinsed in PBS, exposed to a donkey anti-goat IgG conjugated to Alexa Fluor 488 for 1 h at RT, and mounted in VECTASHIELD Hard-Set Mounting Medium (Vector).

The biocytin contained in the patch-clamp-recorded neurons was revealed with FITC 488–conjugated extravidin (1:300; Sigma) in PBS solution for 1 h at RT. To investigate the expression of paired-like homeobox 2b (Phox2b) transcription factor, neurokinin 1 receptors (NK1R), and the motor neuronal marker Islet, we incubated the preparations with the following primary antibodies: a mouse anti-Phox2b antibody (1:100; Santa Cruz), a rabbit anti-NK1R antibody (1:10000; Sigma), and a mouse anti-Islet antibody (1:250; DSHB). We then used goat anti-rabbit Alexa Fluor 568 or goat anti-mouse Alexa Fluor 488 secondary antibodies. The preparations were incubated with primary antibodies overnight under agitation at RT and with secondary antibodies for 1 h. Processed preparations were mounted in VECTASHIELD Hard-Set, and fluorescence was visualized with a Leica SP5 confocal microscope. The images were color corrected and assembled with the Leica LAS AF Lite viewer and Adobe Illustrator.

## Statistical analysis

Statistic analyses were carried out with SigmaPlot 11.0 (Systat), and results are expressed as mean ± SEM. Student's *t* test was used to compare the means of two groups, and repeated measures ANOVA and subsequent Tukey's post hoc tests were used to compare more than two groups. Differences were considered statistically significant when the value of *P* was <0.05.

## Results

### Pharmacological activation of lumbar CPG increased respiratory frequency

In brainstem-spinal cord preparations, inspiratory- and expiratory-related motor activities recorded from cervical (C4) and lumbar (L2) ventral roots [29,30], respectively, occurred at a low frequency (see Materials and Methods), with a mean value of $1.68 \pm 0.28$ bursts/min in normal aCSF (n = 14 preparations; Fig. 1A and 1E, open bar at left). To elicit prolonged episodes of stable fictive locomotion, we bath-applied a mixture of NMA (15 µM) and 5HT (15 µM) selectively to the lumbosacral cord. In the presence of these neuromodulators, extracellular recordings from right and left L2 and left L5 ventral roots, which preferentially innervate hindlimb flexor and extensor muscles, respectively, showed coordinated rhythmic motor activity (Fig. 1B) characterized by strict left-right and flexor-extensor alternations (Fig. 1D). Strikingly, during these bouts of fictive locomotion, the respiratory burst frequency was 60% higher than the control value ($2.74 \pm 0.28$ bursts/min; $P<0.001$; n = 14 preparations; Fig. 1B and 1E, blue bar). It is noteworthy that in preparations showing a higher baseline respiratory rate (5 bursts/min), we previously reported that pharmacological activation of the lumbar cord still produced a significant 30% respiratory rhythm acceleration [16]. In the present study, this increase was reversible after 30 min of wash out (Fig. 1C and 1E, open bars at right) and was no longer observed when axonal conduction in the thoracic spinal segments (T2–T12) was prevented by means of sucrose blockade (Fig. 1F). These findings strongly suggest that, when active, the hindlimb
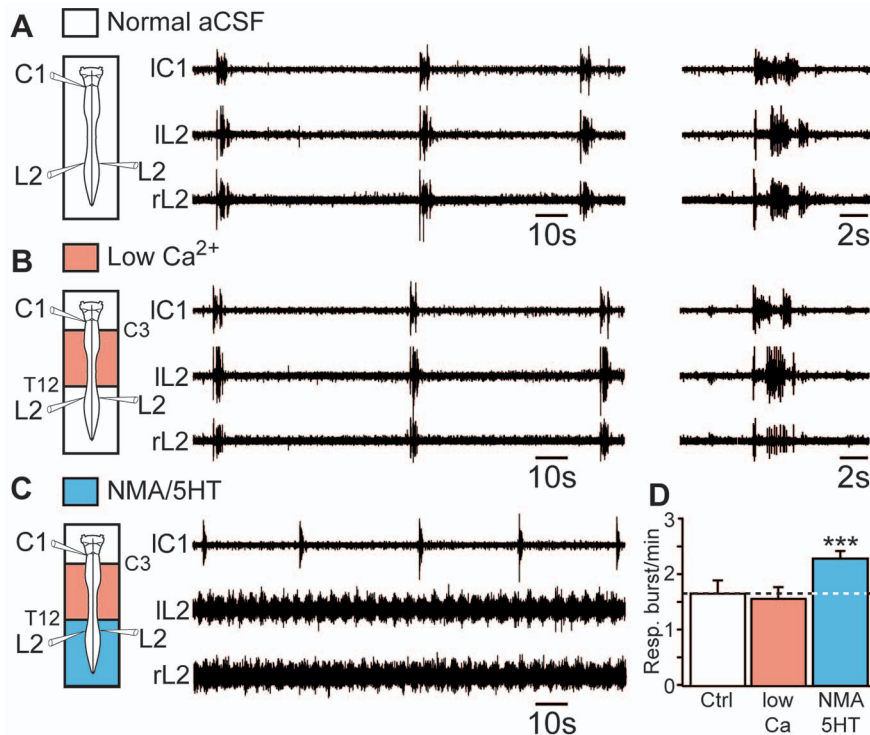
**Figure 4. Excitatory influence of lumbar locomotor networks on respiratory centers does not require supralumbar spinal synaptic relays.** A, B, C, *left*, Schematics of experimental setup. *middle*, Raw spontaneous respiratory activity recorded from cervical (C1, inspiratory-like) and lumbar (L2, expiratory-like) ventral roots under control conditions (A), during the application of a low-$Ca^{2+}$/high-$Mg^{2+}$ saline solution (Low $Ca^{2+}$) to the cervicothoracic (C3–T12) segments (B), and during subsequent activation of the lumbar locomotor CPG with a mixture of NMA and 5HT (C). Note that the respiratory pattern remained unchanged after the pharmacological blockade of cervicothoracic synaptic transmission (expanded traces at right in A and B) with the low-$Ca^{2+}$/high-$Mg^{2+}$ saline solution. D, Bar charts illustrating changes in respiratory burst frequency (Resp.) under these 3 experimental conditions (mean ± SEM; n = 8 preparations). Recordings shown in A to C are from the same preparation. Ctrl, control conditions. ***$P <$ 0.001 (repeated measures ANOVA, Tukey's post hoc tests).
doi:10.1371/journal.pone.0089670.g004

locomotor CPG exerted an excitatory ascending influence on the medullary respiratory rhythm generators.

During locomotion, lumbar CPG rhythmically produces time-dependent excitation phases at the origin of locomotor bursting. We assumed, therefore, that the caudorostral influence from the lumbar locomotor network to the respiratory centers should be maximal during the generation of a locomotor burst activity. Indeed, during episodes of stable fictive locomotion, a clear locomotor-respiratory temporal relationship occurred, which consisted of an in-phase relationship between C4 respiratory and ipsilateral L2 locomotor bursts (Fig. 2A and 2B). The respiratory burst onset invariably occurred during the first 20% of the locomotor cycle and shortly after lumbar locomotor burst onset (mean delay 370±47 ms; n = 57 motor bursts from 8 preparations; Fig. 2B). Finally, this in-phase relationship was no longer observed when lumbar locomotor CPG and medullary respiratory generators were disconnected by sucrose blockade of thoracic (T2–T12) spinal segments (n = 8; Fig. 2C and 2D). These data show that the central modulation of respiratory center burst activity by locomotor networks can contribute to the coupling between breathing and locomotor rhythms.

## Sacrocaudal afferent stimulation-induced fictive locomotion caused increased respiratory rhythmicity

Tonic electrical stimulation of sacrocaudal afferents (SCA) is an alternative, drug-free method of activating lumbar locomotor CPG [31–33]. SCA stimulation also induced a rhythmic locomotor-like

activity recorded in left and right L2 ventral roots (Fig. 3B and 3C), characterized by bilateral burst alternation (n = 7 preparations; Fig. 3D). Similar to the effect observed after pharmacological activation of the lumbar cord, a significant increase in respiratory burst frequency occurred during SCA stimulation (1.61±0.23 bursts/min under control conditions vs 3.62±0.36 bursts/min during SCA stimulation; P<0.001; n = 7 preparations; Fig. 3A, 3B and 3E) and could extend for several tens of seconds after the end of stimulation (Fig. 3B). These findings further support the conclusion that the activation of locomotor CPG in the lumbar region can modulate the activity of respiratory rhythm generators.

## Pathways mediating locomotion-induced modulation of respiratory rhythm

In the context of quadrupedal locomotion, four-limb coordination relies on a powerful caudorostral synaptic influence that originates from the lumbar locomotor CPG and reaches the cervical cord level through activation of intervening thoracic segments [34]. To determine whether the increase in respiratory burst frequency evoked during lumbar fictive locomotion was also mediated by synaptically relayed ascending pathways, we blocked chemical synaptic transmission in thoracic and cervical segments with a low-$Ca^{2+}$/high-$Mg^{2+}$ medium and simultaneously activated the lumbosacral cord with a combination of NMA and 5HT. First, the blockade of chemical synaptic transmission in spinal segments extending from C3 to T12 altered neither the frequency of the ongoing respiratory rhythm (1.62±0.25 bursts/min under control
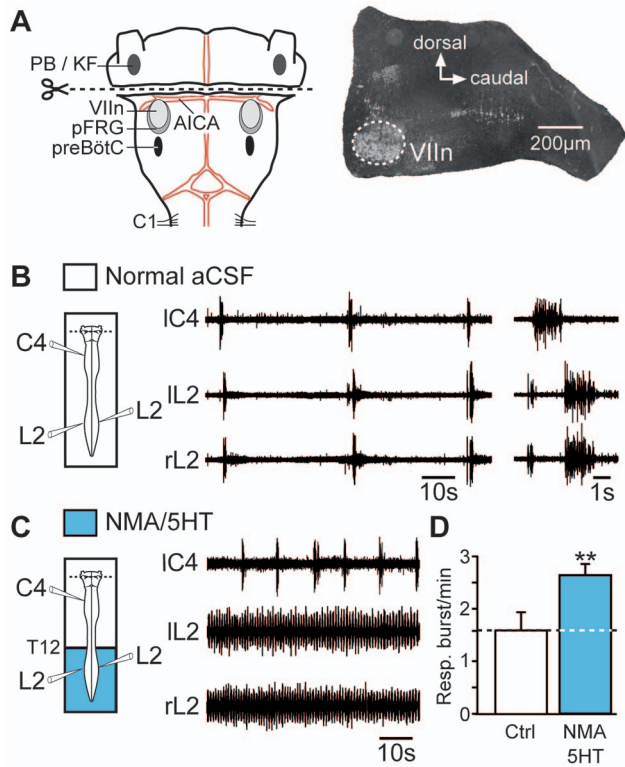
**Figure 5. Pontine structures are not engaged in the accelerated respiration induced by activation of the lumbar locomotor CPG.** A, *left*, Schematic drawing showing the level of transection (dotted line) performed rostral to the AICA. Note that this transection allowed removal of pontine structures of the brainstem while preserving medullary nuclei. *right*, Histological control of the brainstem transection. The parasagittal section, which was immunostained for acetylcholinesterase, clearly shows the transection rostral to the facial nucleus (VIIn). B, C, *left*, Schematic of experimental procedures. *middle*, Raw spontaneous respiratory activity recorded from cervical (C4, inspiratory-like) and left (l) and right (r) lumbar (L2, expiratory-like) ventral roots under control conditions (B, with expanded traces shown at right) and during the pharmacological activation of the lumbar locomotor generators with NMA/5HT (C). D, Bar charts showing changes in respiratory burst frequency (Resp.; mean ± SEM; n = 7 preparations) under control saline conditions (open bar) and during NMA/5HT application to the lumbar spinal region (blue bar). Ctrl, control conditions; PB/KF, parabrachial/Kölliker–Fuse complex. **$P < 0.01$ (Student's paired $t$ test).
doi:10.1371/journal.pone.0089670.g005

conditions *vs* 1.53±0.22 bursts/min under blockade conditions; n = 8 preparations; Fig. 4A, 4B and 4D) nor the pattern of inspiratory and expiratory phases recorded from cervical (C1) and lumbar (L2) ventral roots, respectively (Fig. 4A and 4B, expanded traces on right). Second, when fictive locomotion was subsequently pharmacologically induced in the lumbar cord region, the respiratory rhythm frequency was significantly increased (2.25±0.14 bursts/min; $P < 0.001$; n = 8 preparations; Fig. 4C and 4D). We therefore propose that the influence of the hindlimb locomotor CPG on the respiratory centers relies on nonrelayed ascending supralumbar spinal pathways.

## Pontine structures are not involved in the acceleration of respiration induced by activation of lumbar locomotor CPG

In an attempt to identify supraspinal structures engaged in the modulation of respiratory rhythmicity, a series of transections was made just rostral to the AICA to remove pontine structures (n = 7 preparations; Fig. 5A), including the parabrachial/Kölliker-Fuse complex, which is known to play a crucial role in locomotor-respiratory couplings [17,18]. In this medullary preparation, a normal respiratory-related activity pattern was maintained (Fig. 5B), showing inspiratory and expiratory phases monitored from C4 and L2 ventral roots, respectively (Fig. 5B, expanded traces on right). We also observed that the pharmacological induction of locomotor-like activity in the lumbar cord networks significantly increased the frequency of spontaneous respiratory rhythm (1.58±0.34 bursts/min under control conditions *vs* 2.62±0.21 bursts/min under pharmacological induction; $P < 0.01$; n = 7 preparations; Fig. 5C and 5D), as previously observed in pontomedullary preparations. These results demonstrate that pontine structures are not required for the modulation of respiratory rhythm by the lumbar locomotor CPG.

## Lumbar modulation of respiratory rhythm required functional parafacial respiratory groups

The above finding supports the conclusion that ascending influence from lumbar locomotor CPG has access to medullary structures engaged in the modulation of respiratory rhythmic activity. It is now widely admitted that respiratory rhythm is generated by two distinct but functionally interacting rhyhtmo-genic oscillators, the parafacial respiratory group (pFRG) and the pre-Bötzinger complex (preBötC; for review see [[35]). Because we previously reported that pFRG-driven lumbar expiratory activity was first evoked during respiratory entrainment by limb proprioceptive afferents in the neonate [18], we investigated here the potential involvement of pFRG in the caudorostral influence of locomotor CPG on central respiratory networks. We conducted experiments combining direct electrophysiological recording of pFRG activity and subsequent mechanical bilateral lesions of the pFRG region. Extracellular recording performed in the pFRG region showed pre- and post-inspiratory discharges (Fig. 6A) occurring in a typical double bursting pattern [29,36] responsible for the respiratory lumbar nerve activity [25,29,30]. With intact (Fig. 6B and 6C) and functionally active pFRG network (Fig. 6E), activation of lumbar locomotor generators (Fig. 6F and 6G) resulted in a significant increase in respiratory burst frequency (1.44±0.21 bursts/min under control conditions *vs* 2.44±0.46 bursts/min; $P < 0.01$; n = 7 preparations; Fig. 6H). After the bilateral lesion of pFRG network, which was corroborated by the loss of bursting in L2 ventral root recordings (Fig. 6J) and verified histologically (Fig. 6I), the ability of hindlimb locomotor CPG to modulate the central respiratory burst frequency was abolished (n = 7; Fig. 6K and 6L). Taken together, these results provide evidence that in the neonatal rat, neural components of the pFRG network are involved in the upward influence exerted by the lumbar CPG on respiratory centers during episodes of fictive locomotion.

## Cellular and neuromodulatory mechanisms for locomotor-respiratory network coordination

We next examined the cellular mechanisms underlying the locomotion-induced increase in respiratory rate. Using a preparation (adapted from [36]) giving direct access to the parafacial region at the cut surface of the transection (Fig. 7A), whole-cell patch-clamp recordings were performed from pFRG neurons (n = 10 cells) in current-clamp mode. Located ventral to the facial motor nucleus and close to the ventral surface of the brainstem, pFRG/Pre-I neurons displayed spontaneous periodic membrane depolarizations characterized by the presence of pre- and
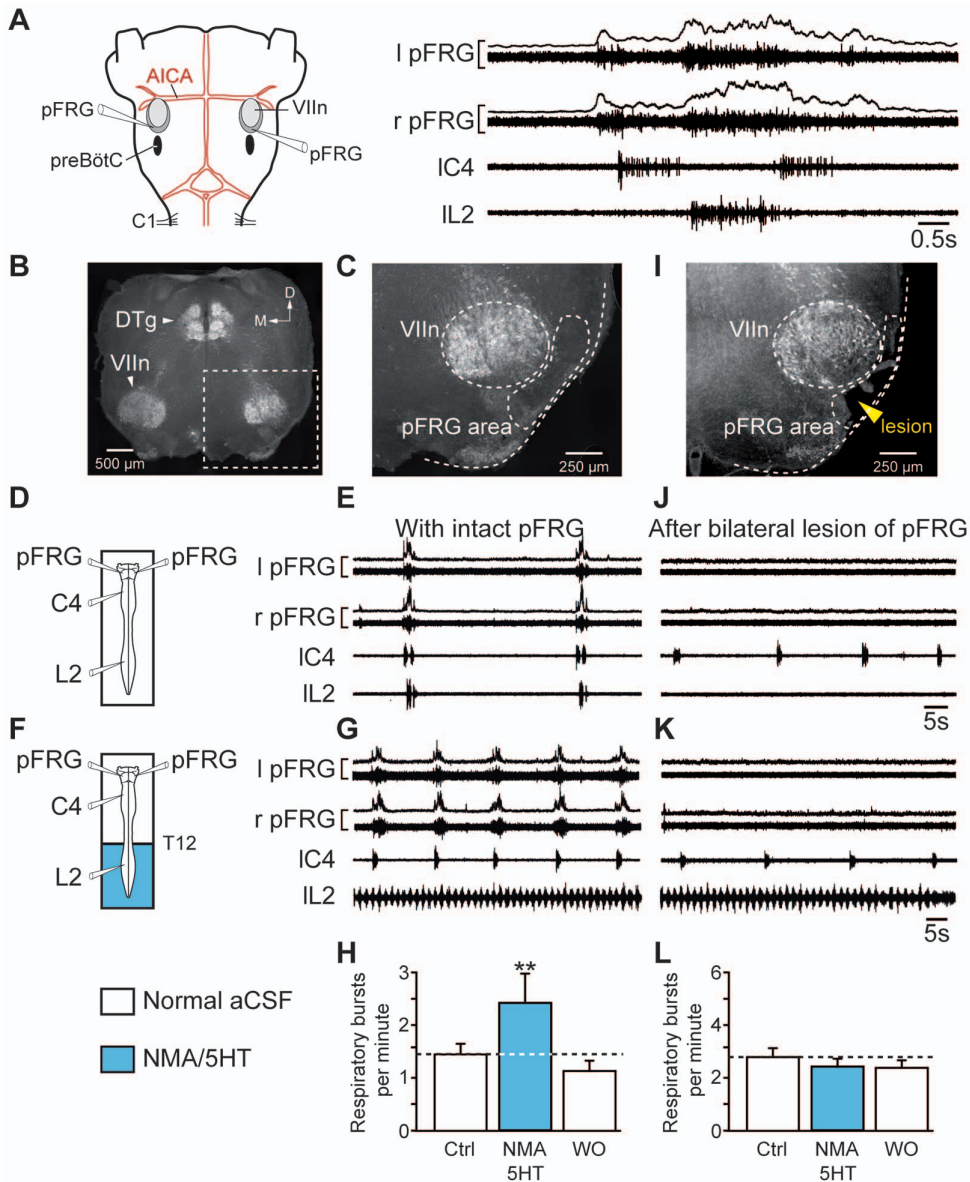
**Figure 6. Bilateral lesion of the pFRG suppresses the locomotion-induced accelerated respiration.** A, *left*, Representation of the brainstem–spinal cord preparation with medullary recording sites. *right*, Averaged integrated (6 sweeps) and raw respiratory burst activity recorded from the left (l) and right (r) pFRG and from spinal (cervical C4 and lumbar L2) ventral roots. B, C, I, Transverse acetylcholinesterase-stained sections as histological control in intact (B, C) and lesioned (I) brainstem preparations. The position of the lesion ventral to the facial motor nucleus corresponds to the location of the pFRG (I). D, F, Schematics of experimental setup. E, J, Spontaneous respiratory activity recorded bilaterally from the pFRG and homolaterally from cervical (C4) and lumbar (L2) ventral roots under control conditions in intact preparation (E) and after the bilateral lesion of the pFRG (J). G, K, Respiratory effects of lumbar cord activation with NMA/5HT in intact (G) and pFRG-lesioned (K) brainstem-spinal cord preparations. H, L, Bar charts showing variation in the respiratory burst frequency (Resp.; mean ± SEM) under control conditions (open bar, left), during pharmacological activation of lumbar locomotor CPG (blue bar), and after wash-out (open bar, right) in intact (H, n = 7 preparations) and pFRG-lesioned (L, n = 7 preparations) preparations. Recordings shown in E, G, J and K are from the same preparation. VIIn, facial motor nucleus; Ctrl, control conditions; DTg, dorsal tegmental nucleus; D, dorsal; M, medial; WO, wash-out. **$P < 0.01$ (repeated measures ANOVA, Tukey's post hoc tests).
doi:10.1371/journal.pone.0089670.g006

post-inspiratory discharges (Fig. 7B1) and were immunoreactive for the transcription factor Phox2b (n = 6/6 cells; Fig. 7B2), as previously described [37,38]. Activation of lumbar locomotor networks by NMA/5HT-containing saline induced a tonic depolarization of pFRG/Pre-I neurons by $6.1 \pm 1.3$ mV (n = 10 neurons; Fig. 7C). This membrane depolarization, which was partially reversible ($3.2 \pm 0.7$ mV; n = 6 neurons), was associated with an increase in action potential firing, indicating a general

increase of pFRG/Pre-I neuron excitability during drug-evoked fictive locomotion in the lumbar spinal cord.

Previous studies have shown that Phox2b-immunoreactive cells in the parafacial region also express NK1R [38–40] and that pFRG/Pre-I neurons are depolarized by the NK1R agonist SP [41]. Therefore, in a final series of experiments, we investigated the possibility that a release of SP in the medulla was involved in the respiratory burst frequency acceleration that results from the activation of lumbar locomotor CPG. First, NK1R was expressed
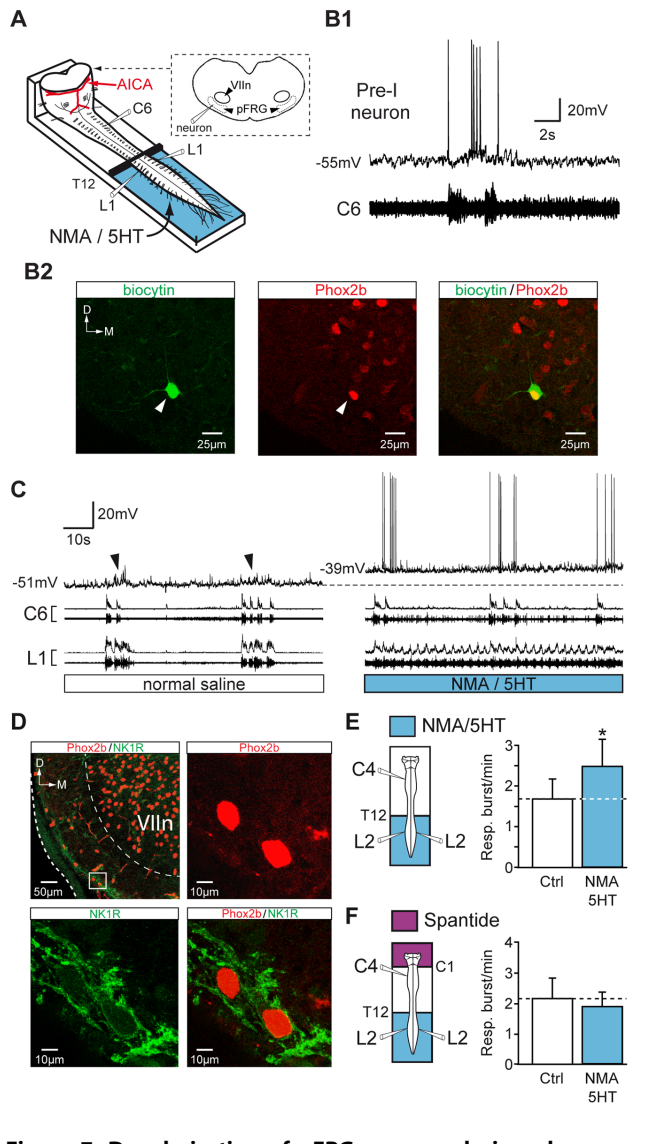
**Figure 7. Depolarization of pFRG neurons during pharmacologically induced locomotion in the lumbar spinal cord: involvement of an SP pathway.** A, Schematic representation of the preparation. The brainstem was transected rostrally to the AICA to allow direct access to pFRG neurons for patch-clamp recording. B1, Simultaneous whole-cell patch-clamp recording of a pFRG/Pre-I neuron and raw activity of the cervical (C6, inspiratory-like) ventral root under control conditions. B2, Photomicrographs (z-stack of 3 images, 1.8 μm in total thickness) of immunolabeling for Phox2B (middle, red) in a biocytin-filled neuron (left, green). The white arrowhead indicates the neuron recorded in B1, and the merged image (right) confirms that the double-labeled (yellow) cell was a functionally identified Pre-I neuron. The dashed line shows the ventrolateral edge of the medulla. C, Simultaneous whole-cell patch-clamp recording of a pFRG/Pre-I neuron (black arrowhead indicating spontaneous rhythmic respiratory depolarization) and integrated and raw activity of cervical (C6) and lumbar (L1) ventral roots under control saline conditions (left) and during NMA/5HT application to lumbar region (right). The dashed line indicates the resting membrane potential level under control conditions. D, Left, top, Distribution of NK1R (green) immunoreactivity and Phox2B-positive cells (red) in the ventrolateral part of the medulla (this photomicrograph corresponds to a z-stack of 18 images, 18 μm in total thickness). The inset (white rectangle) shows the ventrolateral aspect of the VIIn at a higher magnification. Note that cells located in the area corresponding to the pFRG networks are immunopositive for Phox2b (right, top, red; z-stack of 3 images, 2.4 μm in total thickness) and for NK1R (left, bottom, green), as confirmed by the merged image (right, bottom). E, F,

*left*, Schematics of experimental procedures. *right*, Bar charts showing variation in the respiratory burst frequency (Resp.; mean ± SEM) under control saline conditions (open bar) and during NMA/5HT application to the lumbar spinal cord (blue bar) during perfusion of the brainstem with normal saline (E, n = 7 preparations) or with a medium containing the SP antagonist spantide (F, n = 7 preparations). Ctrl, control conditions; D, dorsal; M, medial. *P<0.05 (Student's paired *t* test).
doi:10.1371/journal.pone.0089670.g007

in the area where patch-clamp recordings were performed, ventrally to the facial motor nucleus (Fig. 7D, upper left microphotograph). Moreover, we confirmed that Phox2b-immunoreactive neurons of the pFRG also expressed NK1R (Fig. 7D). Second, we investigated whether the respiratory burst frequency modulation produced by locomotor CPG was mediated by a SP-releasing pathway. The significant increase in respiratory burst frequency evoked during fictive locomotion in response to NMA/5HT activation of lumbar cord (1.70±0.49 bursts/min under control conditions *vs* 2.47±0.67 bursts/min during fictive locomotion; P<0.05; n = 7 preparations; Fig. 7E) was no longer observed when the brainstem was selectively exposed to the NK1R antagonist spantide (5 μM; n = 7 preparations; Fig. 7F). These results support the conclusion that the ascending influence of the lumbar locomotor CPG activates the release of SP, which in turn leads to the acceleration of the breathing rate.

## Discussion

The results described in this report provide evidence indicating that lumbar locomotor pattern generators can participate to the modulation of respiratory network activity during episodes of locomotion. The modulation is mediated by ascending excitatory information that is conveyed to central respiratory networks through an SP-releasing pathway within the brainstem. During activation of hindlimb locomotor CPGs, pFRG/Pre-I neurons are tonically depolarized and show a global excitability increase that could be part of neurogenic mechanisms responsible for accelerating breathing rate during locomotion. Our findings suggest that in addition to playing a role in respiratory rhythm generation and central chemoreception [35,41,42], pFRG/Pre-I neurons also appear to be engaged in the interaction between locomotor and respiratory neural networks.

### A spinal efference copy signal to modulate respiratory network activity

It is now widely recognized that spinal locomotor networks are continuously controlled by several brainstem centers and descending pathways [43–45] that in turn receive ascending feedback information arising from both peripheral sensory systems and spinal locomotor CPGs [46]. Specifically, this CPG-derived efference copy, which is part of a spino-bulbo-spinal loop in the lamprey [47] and spinocerebellar tracts in the cat [48], strongly contributes to rhythmic activity in reticulospinal [49–51] and vestibulospinal neurons [52], thereby actively participating in the adaptation of the locomotor movements and posture during locomotion. At the spinal level, this locomotor-related efference signal also appears to be essential for coordinating back and limb muscle contractions during appendicular swimming or quadrupedal walking. For instance in *Xenopus* froglets, postural adjustments are mediated by projections that ascend from the hindlimb lumbar CPG to the thoracic spinal circuitry controlling the trunk musculature [53]. Similarly, in neonatal rats, lumbar locomotor CPG-related commands have been found to coordinate trunk curvature with hindlimb stepping [54] and also to contribute to interlimb coordination during locomotion by means of coupling

between the lumbar pattern generator and its cervical counterpart [24,34].

It is noteworthy that during locomotion, these ascending copies of lumbar output can also assist distant neural networks engaged in different rhythmic motor behaviors. Indeed, ascending efference copies of rhythmic activities produced by the locomotor CPG within the lumbar cord of *Xenopus* tadpoles [55,56] and frogs [57] have recently been reported to target the brainstem extraocular motor nuclei to help stabilize gaze during undulatory and appendicular swimming, respectively. Our results show that CPG-derived efference copies can also be engaged in the remote control of respiratory rhythm-generating networks. Compatible with feedforward mechanisms to rapidly accelerate the rate of respiratory movements at the onset of exercise [9], the ascending spinal influence could also participate to the emergence of a locomotor-respiratory coupling. Indeed, we report here that an in-phase relationship occurs between locomotor and respiratory burst activity, a phenomenon that could assist the locomotor-respiratory coupling generated by the rhythmic activation of limb proprio-ceptive afferents during locomotion [16,18]. Finally, we demon-strate that the transmission of the lumbar CPG-derived influence to the respiratory centers is mediated mainly by direct spinal ascending nerve tracts, rather than by polysynaptic pathways. A similar anatomical organization, involving a direct spinal ascend-ing pathway, has also been reported for gaze stabilization during locomotion in *Xenopus* [56,57]. In these studies, the drive signals from the spinal locomotor CPG are directly targeted to extraocular motoneurons during swimming. We hypothesize that this direct connectivity promotes rapid, efficient coordination between two otherwise functionally and anatomically distinct motor systems.

## pFRG/Pre-I neurons: new "motion sensors" in locomotor-respiratory coordination?

The last decade of research on central respiratory circuits has provided several lines of evidence showing that the pFRG contributes to the rhythmogenesis of respiration during the perinatal period in rodents [36,38,58,59], contributes to the production of active expiration [25,30,60,61], and plays a major role in central chemoreception [40,62–68]. Here, our lesion and patch-clamp experiments demonstrate for the first time that the pFRG cell population is also implicated in the locomotor-respiratory interaction. In this context, pFRG/Pre-I neurons may convert the lumbar CPG-derived efference copy into excitatory signals, which would be subsequently transmitted to the whole respiratory network. Indeed, the functional connections that exist between the pFRG and other crucial respiratory nuclei [69,70] allow the widespread transmission of these excitatory inputs in other neuronal groups involved in the genesis or the modulation of respiratory rhythm. Interestingly, this functional

organization closely resembles the one implicated in central mechanisms for chemosensitivity. Indeed, the increase in respira-tory rate observed during acidosis [71] is likely due to the excitation of pFRG neurons [40,62,67] because *in vitro*, the preBötC, known to be responsible for generating inspiration phase [72], is not intrinsically sensitive to pH changes [65].

In our experiments, the acceleration of respiratory rhythm during locomotion was suppressed when the brainstem was initially exposed to spantide, an NK1R antagonist. As previously reported in rodents [38–40] and in humans [73], we show that Phox2b-positive neurons in the pFRG region also express NK1R. Therefore, SP that is co-localized with serotonin in terminals located in the pFRG [39] and is known to excite pFRG/Pre-I neurons [41,67,74] is suspected to play a role in pFRG/Pre-I cell depolarization induced by the lumbar CPG during locomotion. Although its precise contribution to the process of coordination remains undetermined, this SP-dependent link would contribute to the transformation of a phasic ascending input from the lumbar locomotor CPG into a tonic excitatory signal. Consequently, the long-lasting depolarization of pFRG/Pre-I neurons, which acti-vates their burst-generating mechanisms, could therefore underlie the rapid adjustment of breathing rate that occurs at the onset of exercise.

Does ascending influence from the lumbar locomotor CPG stimulate the preBötC? An action of SP on the preBötC neurons during locomotion cannot be completely ruled out. Indeed, NK1R is strongly expressed in the preBötC region [75–78], and exposure of the preBötC network to SP evokes in inspiratory neurons a membrane depolarization [75,79] or a voltage-insensitive inward current [80] leading to an increase in the respiratory frequency [28,75,79,81]. But after bilateral lesions that removed the pFRG and left intact the preBötC, we demonstrated that the ability of lumbar CPG to modulate the respiratory rhythmicity was clearly abolished. These results tend to suggest that the pFRG would be the main oscillator directly engaged in the lumbar locomotor CPG-induced increase in respiratory rate. In any case, further experiments are required to fully elucidate the exact role of preBötC neurons in the functional interaction between the locomotor and respiratory CPGs.

## Acknowledgments

## Author Contributions

Conceived and designed the experiments: JPLG DM. Performed the experiments: JPLG LJ LC MTB. Analyzed the data: JPLG LC MTB. Wrote the paper: JPLG LJ MTB DM.

## References

1. Mateika JH, Duffin J (1995) A review of the control of breathing during exercise. Eur J Appl Physiol Occup Physiol 71: 1–27.
2. Haouzi P, Hirsch JJ, Marchal F, Huszczuk A (1997) Ventilatory and gas exchange response during walking in severe peripheral vascular disease. Respir Physiol 107: 181–190.
3. Tobin MJ, Perez W, Guenther SM, D'Alonzo G, Dantzker DR (1986) Breathing pattern and metabolic behavior during anticipation of exercise. J Appl Physiol 60: 1306–1312.
4. Gravel J, Brocard F, Gariepy JF, Lund JP, Dubuc R (2007) Modulation of respiratory activity by locomotion in lampreys. Neuroscience 144: 1120–1132.
5. Bell HJ (2006) Respiratory control at exercise onset: an integrated systems perspective. Respir Physiol Neurobiol 152: 1–15.
6. Gariepy JF, Missaghi K, Dubuc R (2010) The interactions between locomotion and respiration. Prog Brain Res 187: 173–188.
7. Eldridge FL, Millhorn DE, Waldrop TG (1981) Exercise hyperpnea and locomotion: parallel activation from the hypothalamus. Science 211: 844–846.
8. Waldrop TG, Iwamoto GA (2006) Point: supraspinal locomotor centers do contribute significantly to the hyperpnea of dynamic exercise. J Appl Physiol 100: 1077–1079.
9. Gariepy JF, Missaghi K, Chevallier S, Chartre S, Robert M, et al. (2012) Specific neural substrate linking respiration to locomotion. Proc Natl Acad Sci U S A 109: E84–92.
10. Romaniuk JR, Kasicki S, Kazennikov OV, Selionov VA (1994) Respiratory responses to stimulation of spinal or medullary locomotor structures in decerebrate cats. Acta Neurobiol Exp (Wars) 54: 11–17.
11. Duysens J, Clarac F, Cruse H (2000) Load-regulating mechanisms in gait and posture: comparative aspects. Physiol Rev 80: 83–133.
12. Pearson K (2000) Motor systems. Curr Opin Neurobiol 10: 649–654.

13. Iscoe S, Polosa C (1976) Synchronization of respiratory frequency by somatic afferent stimulation. J Appl Physiol 40: 138–148.

14. Kawahara K, Kumagai S, Nakazono Y, Miyamoto Y (1988) Analysis of entrainment of respiratory rhythm by somatic afferent stimulation in cats using phase response curves. Biol Cybern 58: 235–242.

15. Funk GD, Milsom WK, Steeves JD (1992) Coordination of wingbeat and respiration in the Canada goose. I. Passive wing flapping. J Appl Physiol 73: 1014–1024.

16. Morin D, Viala D (2002) Coordinations of locomotor and respiratory rhythms in vitro are critically dependent on hindlimb sensory inputs. J Neurosci 22: 4756–4765.

17. Potts JT, Rybak IA, Paton JF (2005) Respiratory rhythm entrainment by somatic afferent stimulation. J Neurosci 25: 1965–1978.

18. Giraudin A, Le Bon-Jego M, Cabirol MJ, Simmers J, Morin D (2012) Spinal and pontine relay pathways mediating respiratory rhythm entrainment by limb proprioceptive inputs in the neonatal rat. J Neurosci 32: 11841–11853.

19. Boggs DF (2002) Interactions between locomotion and ventilation in tetrapods. Comp Biochem Physiol A Mol Integr Physiol 133: 269–288.

20. Smith JC, Feldman JL (1987) In vitro brainstem-spinal cord preparations for study of motor systems for mammalian respiration and locomotion. J Neurosci Methods 21: 321–333.

21. Hayes HB, Chang YH, Hochman S (2009) An in vitro spinal cord-hindlimb preparation for studying behaviorally relevant rat locomotor function. J Neurophysiol 101: 1114–1122.

22. Hagglund M, Borgius L, Dougherty KJ, Kiehn O (2010) Activation of groups of excitatory neurons in the mammalian spinal cord or hindbrain evokes locomotion. Nat Neurosci 13: 246–252.

23. Antri M, Mellen N, Cazalets JR (2011) Functional organization of locomotor interneurons in the ventral lumbar spinal cord of the newborn rat. PLoS One 6: e20529.

24. Juvin L, Le Gal JP, Simmers J, Morin D (2012) Cervicolumbar coordination in mammalian quadrupedal locomotion: role of spinal thoracic circuitry and limb sensory inputs. J Neurosci 32: 953–965.

25. Ruangkittisakul A, Secchia L, Bornes TD, Palathinkal DM, Ballanyi K (2007) Dependence on extracellular Ca2+/K+ antagonism of inspiratory centre rhythms in slices and en bloc preparations of newborn rat brainstem. J Physiol 584: 489–508.

26. Panaitescu B, Ruangkittisakul A, Ballanyi K (2010) Depression by Ca2+ and stimulation by K+ of fictive inspiratory rhythm in newborn rat brainstem slices. Adv Exp Med Biol 669: 91–95.

27. Richards CD, Sercombe R (1970) Calcium, magnesium and the electrical activity of guinea-pig olfactory coex in vitro. J Physiol 211: 571–584.

28. Telgkamp P, Cao YQ, Basbaum AI, Ramirez JM (2002) Long-term deprivation of substance P in PPT-A mutant mice alters the anoxic response of the isolated respiratory network. J Neurophysiol 88: 206–213.

29. Janczewski WA, Onimaru H, Homma I, Feldman JL (2002) Opioid-resistant respiratory pathway from the preinspiratory neurones to abdominal muscles: in vivo and in vitro study in the newborn rat. J Physiol 545: 1017–1026.

30. Giraudin A, Cabirol-Pol MJ, Simmers J, Morin D (2008) Intercostal and abdominal respiratory motoneurons in the neonatal rat spinal cord: spatiotemporal organization and responses to limb afferent stimulation. J Neurophysiol 99: 2626–2640.

31. Lev-Tov A, Delvolve I, Kremer E (2000) Sacrocaudal afferents induce rhythmic efferent bursting in isolated spinal cords of neonatal rats. J Neurophysiol 83: 888–894.

32. Whelan P, Bonnot A, O'Donovan MJ (2000) Properties of rhythmic activity generated by the isolated spinal cord of the neonatal mouse. J Neurophysiol 84: 2821–2833.

33. Etlin A, Finkel E, Mor Y, O'Donovan MJ, Anglister L, et al. (2013) Characterization of sacral interneurons that mediate activation of locomotor pattern generators by sacrocaudal afferent input. J Neurosci 33: 734–747.

34. Juvin L, Simmers J, Morin D (2005) Propriospinal circuitry underlying interlimb coordination in mammalian quadrupedal locomotion. J Neurosci 25: 6025–6035.

35. Mellen NM, Thoby-Brisson M (2012) Respiratory circuits: development, function and models. Curr Opin Neurobiol 22: 676–685.

36. Onimaru H, Homma I (2003) A novel functional neuron group for respiratory rhythm generation in the ventral medulla. J Neurosci 23: 1478–1486.

37. Onimaru H, Homma I (1992) Whole cell recordings from respiratory neurons in the medulla of brainstem-spinal cord preparations isolated from newborn rats. Pflugers Arch 420: 399–406.

38. Thoby-Brisson M, Karlen M, Wu N, Charnay P, Champagnat J, et al. (2009) Genetic identification of an embryonic parafacial oscillator coupling to the preBotzinger complex. Nat Neurosci 12: 1028–1035.

39. Mulkey DK, Rosin DL, West G, Takakura AC, Moreira TS, et al. (2007) Serotonergic neurons activate chemosensitive retrotrapezoid nucleus neurons by a pH-independent mechanism. J Neurosci 27: 14128–14138.

40. Onimaru H, Ikeda K, Kawakami K (2008) CO2-sensitive preinspiratory neurons of the parafacial respiratory group express Phox2b in the neonatal rat. J Neurosci 28: 12845–12850.

41. Onimaru H, Ikeda K, Kawakami K (2009) Phox2b, RTN/pFRG neurons and respiratory rhythmogenesis. Respir Physiol Neurobiol 168: 13–18.

42. Guyenet PG, Mulkey DK (2010) Retrotrapezoid nucleus and parafacial respiratory group. Respir Physiol Neurobiol 173: 244–255.

43. Armstrong DM (1988) The supraspinal control of mammalian locomotion. J Physiol 405: 1–37.

44. Jordan LM (1998) Initiation of locomotion in mammals. Ann N Y Acad Sci 860: 83–93.

45. Matsuyama K, Drew T (2000) Vestibulospinal and reticulospinal neuronal activity during locomotion in the intact cat. I. Walking on a level surface. J Neurophysiol 84: 2237–2256.

46. Arshavsky YI, Berkinblit MB, Fukson OI, Gelfand IM, Orlovsky GN (1972) Origin of modulation in neurones of the ventral spinocerebellar tract during locomotion. Brain Res 43: 276–279.

47. Buchanan JT, Einum JF (2008) The spinobulbar system in lamprey. Brain Res Rev 57: 37–45.

48. Fedirchuk B, Stecina K, Kristensen KK, Zhang M, Meehan CF, et al. (2013) Rhythmic activity of feline dorsal and ventral spinocerebellar tract neurons during fictive motor actions. J Neurophysiol 109: 375–388.

49. Dubuc R, Grillner S (1989) The role of spinal cord inputs in modulating the activity of reticulospinal neurons during fictive locomotion in the lamprey. Brain Res 96: 196–200.

50. Antri M, Fenelon K, Dubuc R (2009) The contribution of synaptic inputs to sustained depolarizations in reticulospinal neurons. J Neurosci 29: 1140–1151.

51. Buchanan JT (2011) Spinal locomotor inputs to individually identified reticulospinal neurons in the lamprey. J Neurophysiol 106: 2346–2357.

52. Bussieres N, Dubuc R (1992) Phasic modulation of vestibulospinal neuron activity during fictive locomotion in lampreys. Brain Res 134: 174–179.

53. Beyeler A, Metais C, Combes D, Simmers J, Le Ray D (2008) Metamorphosis-induced changes in the coupling of spinal thoraco-lumbar motor outputs during swimming in Xenopus laevis. J Neurophysiol 100: 1372–1383.

54. Falgairolle M, Cazalets JR (2007) Metachronal coupling between spinal neuronal networks during locomotor activity in newborn rat. J Physiol 580: 87–102.

55. Combes D, Le Ray D, Lambert FM, Simmers J, Straka H (2008) An intrinsic feed-forward mechanism for vertebrate gaze stabilization. Curr Biol 18: R241–243.

56. Lambert FM, Combes D, Simmers J, Straka H (2012) Gaze stabilization by efference copy signaling without sensory feedback during vertebrate locomotion. Curr Biol 22: 1649–1658.

57. von Uckermann G, Le Ray D, Combes D, Straka H, Simmers J (2013) Spinal efference copy signaling and gaze stabilization during locomotion in juvenile Xenopus frogs. J Neurosci 33: 4253–4264.

58. Janczewski WA, Feldman JL (2006) Distinct rhythm generators for inspiration and expiration in the juvenile rat. J Physiol 570: 407–420.

59. Wittmeier S, Song G, Duffin J, Poon CS (2008) Pacemakers handshake synchronization mechanism of mammalian respiratory rhythmogenesis. Proc Natl Acad Sci U S A 105: 18000–18005.

60. Pagliardini S, Janczewski WA, Tan W, Dickson CT, Deisseroth K, et al. (2011) Active expiration induced by excitation of ventral medulla in adult anesthetized rats. J Neurosci 31: 2895–2905.

61. Feldman JL, Del Negro CA, Gray PA (2013) Understanding the rhythm of breathing: so near, yet so far. Annu Rev Physiol 75: 423–452.

62. Guyenet PG, Mulkey DK, Stornetta RL, Bayliss DA (2005) Regulation of ventral surface chemoreceptors by the central respiratory pattern generator. J Neurosci 25: 8938–8947.

63. Voituron N, Frugiere A, Champagnat J, Bodineau L (2006) Hypoxia-sensing properties of the newborn rat ventral medullary surface in vitro. J Physiol 577: 55–68.

64. Ballanyi K, Ruangkittisakul A, Onimaru H (2009) Opioids prolong and anoxia shortens delay between onset of preinspiratory (pFRG) and inspiratory (preBotC) network bursting in newborn rat brainstems. Pflugers Arch 458: 571–587.

65. Dubreuil V, Thoby-Brisson M, Rallu M, Persson K, Pattyn A, et al. (2009) Defective respiratory rhythmogenesis and loss of central chemosensitivity in Phox2b mutants targeting retrotrapezoid nucleus neurons. J Neurosci 29: 14836–14846.

66. Gestreau C, Heitzmann D, Thomas J, Dubreuil V, Bandulik S, et al. (2010) Task2 potassium channels set central respiratory CO2 and O2 sensitivity. Proc Natl Acad Sci U S A 107: 2325–2330.

67. Onimaru H, Ikeda K, Kawakami K (2012) Postsynaptic mechanisms of CO(2) responses in parafacial respiratory neurons of newborn rats. J Physiol 590: 1615–1624.

68. Wang S, Shi Y, Shu S, Guyenet PG, Bayliss DA (2013) Phox2b-expressing retrotrapezoid neurons are intrinsically responsive to H+ and CO2. J Neurosci 33: 7756–7761.

69. Tan W, Pagliardini S, Yang P, Janczewski WA, Feldman JL (2010) Projections of preBotzinger complex neurons in adult rats. J Comp Neurol 518: 1862–1878.

70. Bochorishvili G, Stornetta RL, Coates MB, Guyenet PG (2012) Pre-Botzinger complex receives glutamatergic innervation from galaninergic and other retrotrapezoid nucleus neurons. J Comp Neurol 520: 1047–1061.

71. Voituron N, Shvarev Y, Menuet C, Bevengut M, Fasano C, et al. (2010) Fluoxetine treatment abolishes the in vitro respiratory response to acidosis in neonatal mice. PLoS One 5: e13644.

72. Smith JC, Ellenberger HH, Ballanyi K, Richter DW, Feldman JL (1991) Pre-Botzinger complex: a brainstem region that may generate respiratory rhythm in mammals. Science 254: 726–729.

73. Rudzinski E, Kapur RP (2010) PHOX2B immunolocalization of the candidate human retrotrapezoid nucleus. Pediatr Dev Pathol 13: 291–299.

74. Shvarev YN, Lagercrantz H, Yamamoto Y (2002) Biphasic effects of substance P on respiratory activity and respiration-related neurones in ventrolateral medulla in the neonatal rat brainstem in vitro. Acta Physiol Scand 174: 67–84.

75. Gray PA, Rekling JC, Bocchiaro CM, Feldman JL (1999) Modulation of respiratory frequency by peptidergic input to rhythmogenic neurons in the preBotzinger complex. Science 286: 1566–1568.

76. Gray PA, Janczewski WA, Mellen N, McCrimmon DR, Feldman JL (2001) Normal breathing requires preBotzinger complex neurokinin-1 receptor-expressing neurons. Nat Neurosci 4: 927–930.

77. Guyenet PG, Wang H (2001) Pre-Botzinger neurons with preinspiratory discharges "in vivo" express NK1 receptors in the rat. J Neurophysiol 86: 438–446.

78. Stornetta RL, Rosin DL, Wang H, Sevigny CP, Weston MC, et al. (2003) A group of glutamatergic interneurons expressing high levels of both neurokinin-1 receptors and somatostatin identifies the region of the pre-Botzinger complex. J Comp Neurol 455: 499–512.

79. Ben-Mabrouk F, Tryba AK (2010) Substance P modulation of TRPC3/7 channels improves respiratory rhythm regularity and ICAN-dependent pace-maker activity. Eur J Neurosci 31: 1219–1232.

80. Hayes JA, Del Negro CA (2007) Neurokinin receptor-expressing pre-botzinger complex neurons in neonatal mice studied in vitro. J Neurophysiol 97: 4215–4224.

81. Johnson SM, Smith JC, Feldman JL (1996) Modulation of respiratory rhythm in vitro: role of Gi/o protein-mediated mechanisms. J Appl Physiol 80: 2120–2133.